In-line electron holography with an atomic focuser source

V. V. Smirnov[1,*] and J. M. Cowley[2]
[1]*Institute of Physics, Saint Petersburg State University, 198504, St. Petersburg, Russia*
[2]*Department of Physics and Astronomy, Arizona State University, Tempe, Arizona 85287-1504*
(Received 25 September 2001; published 23 January 2002)

The resolution that may be achieved in an image formed by reconstruction from an in-line electron hologram, without aberration correction, is governed by the source size. Computer simulations show that ultrahigh resolution, of better than 0.05 nm for 100 keV electrons, may be possible if the electron source is a crossover formed at the exit face of a thin atomic-focuser crystal when electrons from a beam focused in a scanning transmission electron microscope (STEM) instrument are channeled along a line of atoms through the crystal. Simulations also show that, because of the channeling effect, the resolution of the reconstructed image is not degraded by translations or oscillations of the STEM beam by 0.1 nm or more. We suggest a scheme for removing the unwanted background and conjugate image from the reconstructed image by combining the in-line holography with an off-axis mode.

DOI: 10.1103/PhysRevB.65.064109 PACS number(s): 61.14.Nm, 61.14.Lj

I. INTRODUCTION

In the scheme for electron holography originally proposed by Gabor[1,2] the specimen is illuminated from a small source and the intensity distribution of the enlarged ''shadow-image'' or hologram is recorded and used as a basis for reconstruction of the specimen transmission function. If the small source is produced by a short-focus electromagnetic lens, compensation for the spherical aberration of the lens in the reconstruction process may be used as the basis for an improvement of the attainable electron microscope resolution. Gabor's original proposal was for reconstruction by use of light-optical methods. It has been shown that digital recording and reconstruction is a useful alternative[3] and some partial success by this method has been achieved.[4]

In the absence of spherical-aberration correction, the resolution of the reconstructed image is limited to the diameter of the source, as determined by the aberrations and defocus of the electromagnetic lens. An alternative approach to the improvement of electron microscopy resolution is the use of the much smaller source produced by an atomic focuser,[5] with or without aberration correction. It has been shown, for example, that if an electron beam, such as that produced in a scanning transmission electron microscopy (STEM) instrument, operating at 100–200 keV, is focused to a diameter of about 0.2 nm and illuminates the first of a row of atoms passing axially through a thin crystal of gold, the electron beam is effectively channeled along the row of atoms and forms a crossover of diameter 0.03 nm at the exit face of the crystal[6] (see Fig. 1). If such a crossover is used as a source for electron holography, reconstruction from the hologram should give an image of a thin specimen with a resolution of better than 0.05 nm. In this paper, we show simulations of reconstructions from holograms produced in this way, demonstrating the possibility of resolutions of this magnitude.

In practical applications of STEM instruments, a limitation of resolution that is commonly encountered comes from drift of the beam or the specimen or instabilities (e.g., oscillations of the beam produced by stray electric or magnetic fields). It may be thought that such effects would be a serious hindrance to the attainment of the projected resolutions for the in-line holography scheme. However, we show that the channeling of electrons along a line of atoms through a crystal provides an automatic compensation for such effects, to an important extent. A lateral translation of the focused electron beam incident on the crystal by as much as half the crystal lattice spacing has a small effect on the intensity of the output probe but very little effect on its position. Our simulations show that resolutions approaching 0.05 nm can be achieved even when the incident STEM beam has instabilities approaching 0.2 nm.

A well-known difficulty with the reconstruction from an in-line hologram is the presence of the conjugate image, produced because the recorded intensity distribution of the hologram contains an ambiguity in the phase of the object transmission function. Various schemes have been proposed for the suppression of the conjugate image, including the recording of series of holograms with variation of defocus or lateral position of the specimen.[4,7] However, for reconstructions of fine detail in suitably thin specimens, it is often sufficient to record the hologram with a large defect of focus. The conjugate image is then produced with twice this defocus value and consequently forms only a diffuse background.

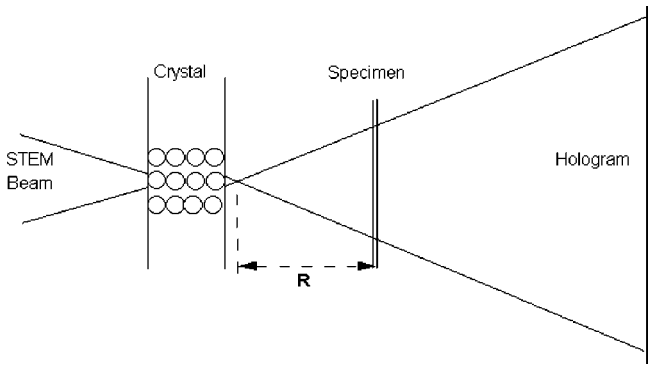

FIG. 1. Diagram of the arrangement for in-line electron holography using a source produced by channeling through an atomic-focuser crystal illuminated by the focused beam from a scanning transmission electron microscope.

If, for example, the distance R from the source to the specimen is 100 nm for 100 keV electrons, the conjugate image has an effective resolution of about $(2R\lambda)^{1/2}$, or 0.8 nm, and should have little effect on the interpretation of the reconstructed image having a resolution of 0.05 nm.

II. THEORY OF RECONSTRUCTION FROM A HOLOGRAM

We consider that the specimen is thin enough to allow the effect on the incident electron beam to be described by a complex transmission function, written as

$$q(x)=1+p(x), \tag{2.1}$$

with the implication that the magnitude of the complex function $p(x)$ is less than unity. For a pure phase object,

$$p(x)=\exp[-i\sigma\varphi(x)]-1, \tag{2.2}$$

and for a weak-phase object $p(x)=-i\sigma\varphi(x)$ is purely imaginary, but in each case real terms arising from absorption effects may be added. For simplicity, we use one-dimensional (1D) functions and ignore multiplicative constants. The extension to two dimensions is trivial.

The amplitude distribution of the small source is written as $t(x)$ which may be considered as the Fourier transform of $T(u)$, the effective transfer function of the atomic-focuser row of atoms, with some influence from the properties of the magnetic lens producing the focused STEM beam illuminating the crystal. The reciprocal space coordinate u has magnitude $2\sin(\phi/2)/\lambda$, where ϕ is the scattering angle. The wave transmitted through the specimen may then be written as

$$\psi(x)=q(x)[t(x)\otimes g(x)],$$

where $g(x)=\exp(-\pi ix^2/R\lambda)$, the vacuum propagator through a distance R between atomic-focuser source and specimen. The amplitude in the plane of the hologram, considered to be at infinity, is given in terms of the Fourier transforms as

$$\Psi(u)=Q(u)\otimes[T(u)\exp(\pi iR\lambda u^2)]$$
$$=\int Q(U)T(u-U)\exp[\pi iR\lambda(u-U)^2]dU.$$

Replacing $Q(u)$ and $T(u-U)$ by their Fourier-transform integrals gives

$$\Psi(u)=\exp(\pi iR\lambda u^2)\int\int\int q(x)t(y)\exp(2\pi iR\lambda uy)$$
$$\times\exp(\pi iR\lambda U^2)\exp[\pi iR\lambda(x-R\lambda u-y]dUdx\,dy.$$

Putting $X=R\lambda u$ and carrying out the integrals over U and y gives

$$\Psi(X)=q(X)\otimes[t(-X)\exp(\pi iX^2/R\lambda)]\otimes\exp(-\pi iX^2/R\lambda).$$

Because the exponential term which is multiplied by $t(X)$ is very broad compared with $t(X)$, it can be ignored. Then the hologram intensity distribution becomes

$$I(X)=|q(X)\otimes t(-X)\otimes\exp(-\pi iX^2/R\lambda)|^2.$$

Application of Eq. (2.1) then gives the separation into terms of zero order, first order, and second order in $p(X)$. The reconstruction is carried out by backpropagating through a distance R, i.e., by convoluting with the function $g^+(x)=\exp(+\pi ix^2/R\lambda)$, to give

$$\Psi_R(X)=1+p(X)\otimes t(-X)+p^*(X)\otimes t^*(-X)$$
$$\otimes\exp(+\pi iX^2/2R\lambda)+\text{second order}. \tag{2.3}$$

We note that the second term gives an image of the object with a resolution approximately equal to the width of the source.

For a weak-phase object the reconstructed image is

$$-i\sigma\varphi(X)\otimes t(-X).$$

The third term represents the complex conjugate of the second term, a distance $-2R$ out of focus.

The process of reconstruction from the hologram is therefore carried out by deconvoluting the hologram intensity distribution by the inverse of the propagation function or by multiplying its Fourier transform by the Fourier transform of the propagation function and backtransforming.

Let us note that the reconstruction procedure may also take some other forms. Thus one can apply convolution or deconvolution with the propagator to the Fourier transform of the hologram. Given that the Fourier transform of an intensity distribution I is well known to be the autocorrelation function of the object,

$$J=\psi^+\otimes\psi,$$

where $+$ represents the complex conjugate with inversion in the plane $x\rightarrow -x$, making simple calculations using the properties of the propagator g, one could write

$$g\otimes J=g(g^+\otimes I).$$

We see that these alternate procedures correspond to one another apart from a factor g, which is not significant for the reconstructed image ($|g|=1$).

So the image may be reconstructed either by deconvoluting the hologram intensity distribution by the backpropagator or else by convoluting the hologram Fourier transform by the propagator.

Application of the backpropagator to the hologram Fourier transform gives the inverted complex conjugate image

$$g^+\otimes J=(g\otimes J)^+. \tag{2.4}$$

III. SIMULATIONS OF RECONSTRUCTIONS

Simulations were made for a 100 keV electron beam with convergence angle 10 mrad. A cross section of the incident electron beam is shown in Fig. 2. The incident wave was propagated through the gold crystal by a multislice algorithm using the multislice package of Kirkland. Crystal thickness was chosen to be 6 nm (15 unit cells). The incident beam was centered on an atomic row in the crystal. In the exit face

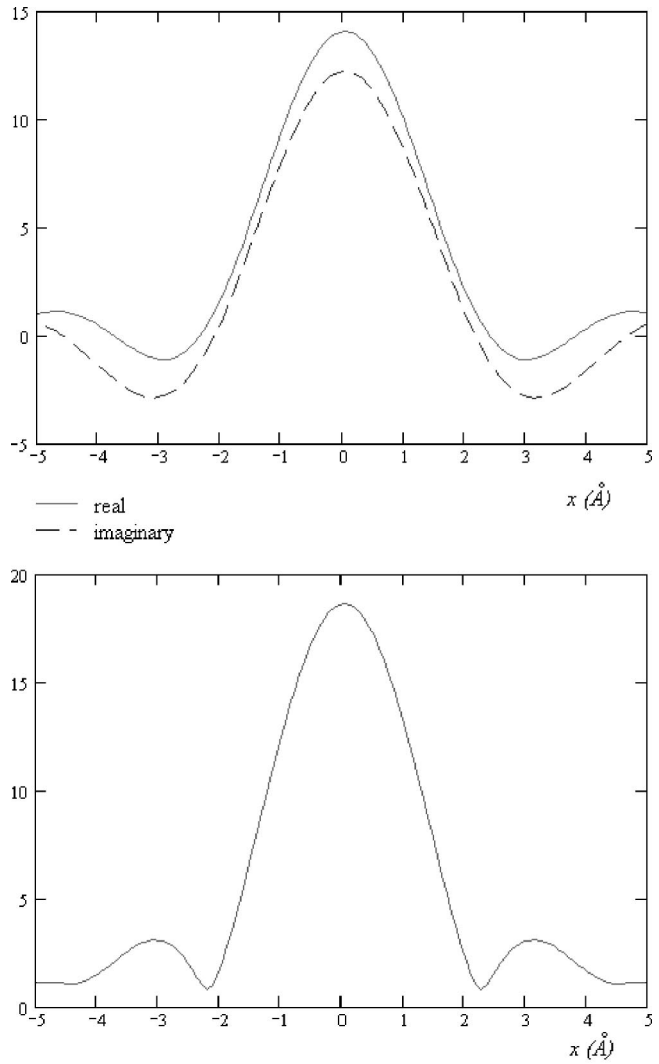

FIG. 2. 1D scan of the incident beam distribution. (a) complex wave, (b) intensity (arbitrary units).

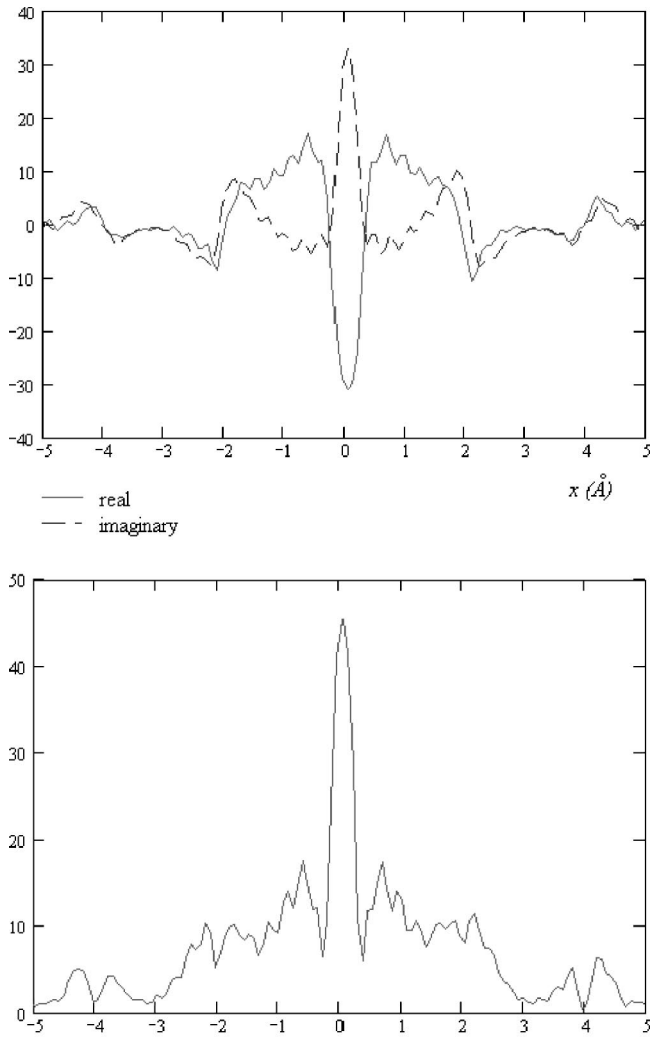

FIG. 3. 1D scan of atomic focuser souce distribution in the exit face of the atomic focuser crystal. (a) complex wave, (b) intensity.

of the crystal we have the atomic-focused beam source with a distribution in cross section shown in Fig. 3.

The specimen was chosen in the form of two scattering centers

$$p(x)=p_0(x-x1)+p_0(x-x2)$$

at a distance $R=20$ nm from the atomic-focuser source, separated by a distance $s=|x1-x2|$. Each center $p_0(x)$ has the form of Eq. (2.2), where $\sigma=\pi/2$ and

$$\varphi(x)=\frac{1}{1+(x/\Delta x)^4},$$

with $\Delta x=0.015$ nm [so that $p(x)$ has both imaginary and real parts].

In order to estimate the resolution, images were reconstructed for various distances and are shown for $s=0.05$ and 0.10 nm.

Figure 4(a) shows the specimen in plan view for the case of $s=0.05$ nm. Figure 4(b) shows the corresponding value of the transmission function p along the line connecting the two centers.

Images were reconstructed by deconvoluting the hologram Fourier transform with the propagator, Eq. (2.4), as described in Sec. II, and hence are inverted and complex conjugated. Figure 5(a) shows the reconstructed image in plan view and Fig. 5(b) the corresponding one-dimensional distribution. Figures 6 and 7 show the same results for a separation between centers, $s=0.10$ nm.

It should be noted that two-dimensional pictures represent only real distributions and hence may appear different when the real and imaginary parts of reconstructed images are shown. The most simple way is to use the modulus of the complex value. But we found that real or imaginary parts give better contrast and further realized that it is better to use some linear combination of the real and imaginary parts in order to obtain maximal visual contrast. This linear combination may be different for different conditions and should be adjusted in each case. In our representation we used the

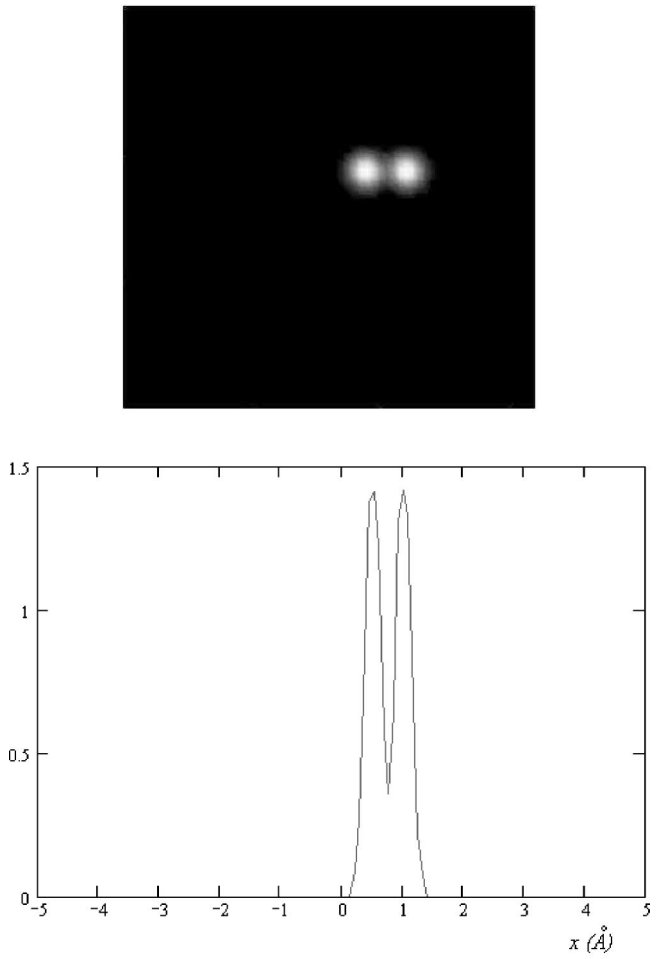

FIG. 4. Specimen with a separation between the centers of 0.05 nm. (a) Intensity distribution in plan view. (b) 1D scan of specimen transmission function p modulus along the line connecting the two centers.

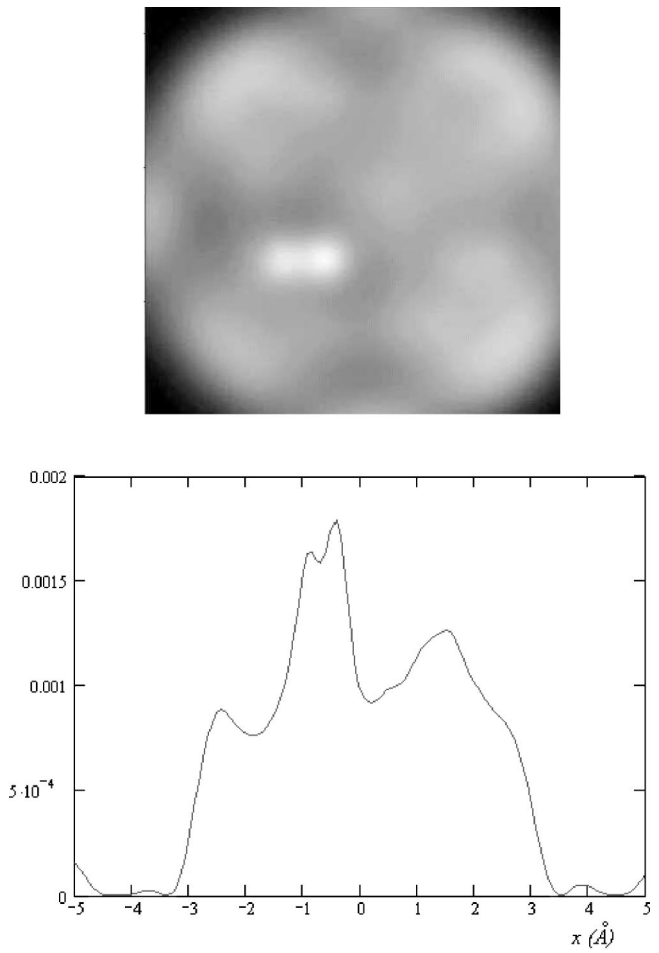

FIG. 5. Reconstructed image corresponding to Fig. 4(a) 2D picture, (b) 1D scan. The diffuse maxima in the background, with separations of about 0.2 nm, come from the third and fourth terms of Eq. (2.3) (the same in Figs. 7, 9, 10, and 12).

second variant of the above procedure. The optimal linear combination in the figures is Re-0.4Im.

The results of the simulations show that a resolution of about 0.05 nm is possible with this atomic-focuser electron holography scheme. This value correlates with atomic-focuser source diameter (Fig. 3). The background from the conjugate image as predicted is out of focus and does not affect image resolution.

IV. SIMULATIONS FOR VARIOUS BEAM DISPLACEMENTS

To study the effect of incident beam drift we made simulations for a set of beam displacements. The incident beam was moved from the central position in the [001] crystal direction by distances 0.025, 0.05, 0.10, and 0.20 nm. The separation of the specimen centers was 0.05 nm.

The simulation results are represented in Figs. 8 and 9. The wave intensity in the exit face of the crystal, i.e., the atomic-focuser source distribution, for each beam position is shown in Fig. 8 and the corresponding reconstructed images are in Fig. 9. The reconstructed images are represented with the optimal linear combination Re-0.4Im.

It is seen that when a drifted incident beam illuminates neighboring atomic rows in the crystal, double atomic-focuser sources and corresponding double images appear, but the beam drift does not affect the resolution.

If the movement of the incident beam does not exceeds half the separation of the atomic rows in the focuser crystal, we have a single reconstructed image.

V. SIMULATIONS FOR AN OSCILLATING BEAM

Random oscillations were simulated by using a set of incident beam positions with a Gausian distribution in the plane of the crystal:

$$\rho(x) = \exp[-(x/\Delta)^2],$$

with a width $\Delta = 0.25$ nm, which may be treated as an average oscillation amplitude.

The hologram is then the sum over this set of partial holograms, giving a corresponding weight for each beam posi-

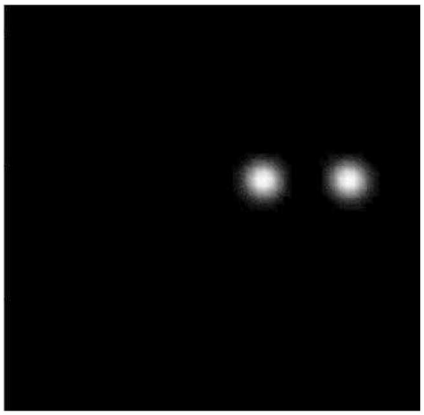

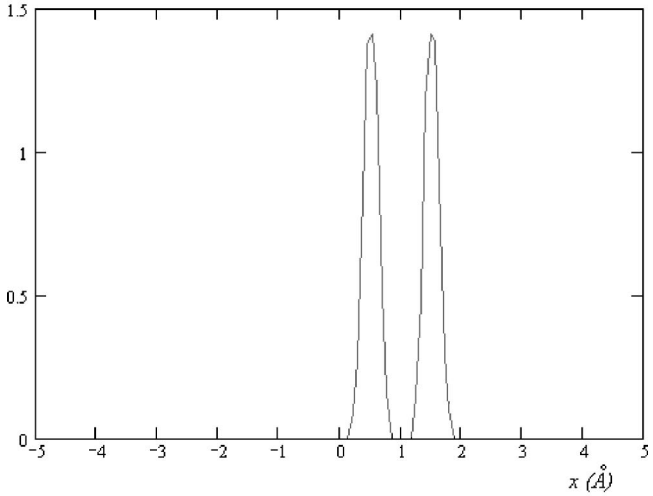

FIG. 6. Specimen with a separation between the centers of 0.10 nm. (a) Intensity distribution in plan view. (b) 1D scan of specimen transmission function p along the line connecting the two centers.

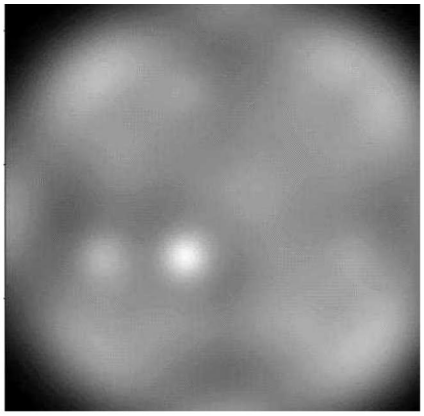

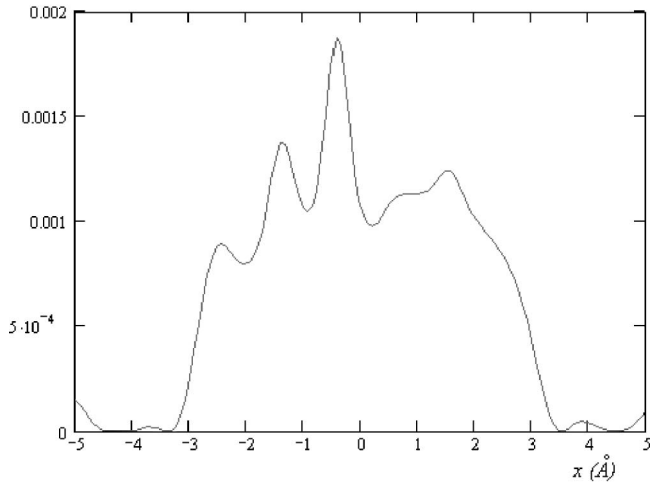

FIG. 7. Reconstructed image corresponding to Fig. 6 (a) 2D picture, (b) 1D scan.

tion. The effective incident beam diameter of 0.5 nm is the sum of the motionless beam diameter and the average oscillation amplitude.

Results of image reconstruction from such a hologram are shown in Fig. 10 with the same contrast optimization as above. Multiple images are seen, with no degradation of the resolution.

VI. SIMULATIONS FOR VARIOUS INCIDENT BEAM CONVERGENCES

The previous results correspond to a broadening of the incident beam by oscillations. They may be compared to the results for a broader motionless beam. We have used incident beam convergence angles of 5 and 4 mrad, corresponding to incident beam diameters of about 0.4 and 0.5 nm.

Whereas the previous sections show the effect of an incoherent addition of intensities from different source points, this section deals with the use of a larger coherent incident beam.

Simulation results are shown in Figs. 11 and 12. The effective multiple sources are shown in Figs. 11(a) and 11(b) for the convergence angles of 5 and 4 mrad, respectively, and the corresponding reconstructed images are shown in Fig. 12. The reconstructions show the multiple images due to the multiple sources, but it is seen that, even with a STEM resolution of no better than 0.4 nm, the reconstruction resolution can approach 0.05 nm.

VII. DISCUSSION AND CONCLUSIONS

The results of the simulations of Figs. 5, 7, 9, 10, and 12 indicate that reconstruction from in-line holograms using an atomic-focuser source can give resolutions of 0.05 nm or better for suitable thin specimens. The simulations of Figs. 9 and 10 suggest that, as a consequence of the channeling effect in the atomic-focuser crystal, the resolution of the reconstructed image is very little affected by movements of the STEM beam that illuminates the crystal focuser. If the STEM instrument used is sufficiently stable to give a normal dark-field resolution of 0.2 nm, a reconstructed image with resolution of 0.05 nm or better should be possible. It is suggested by Fig. 12 that the resolution of the reconstructed image is degraded if the STEM resolution limit is increased by a reduction of the convergence angle by a factor of 2 or more.

The reconstruction depends on only one parameter, the

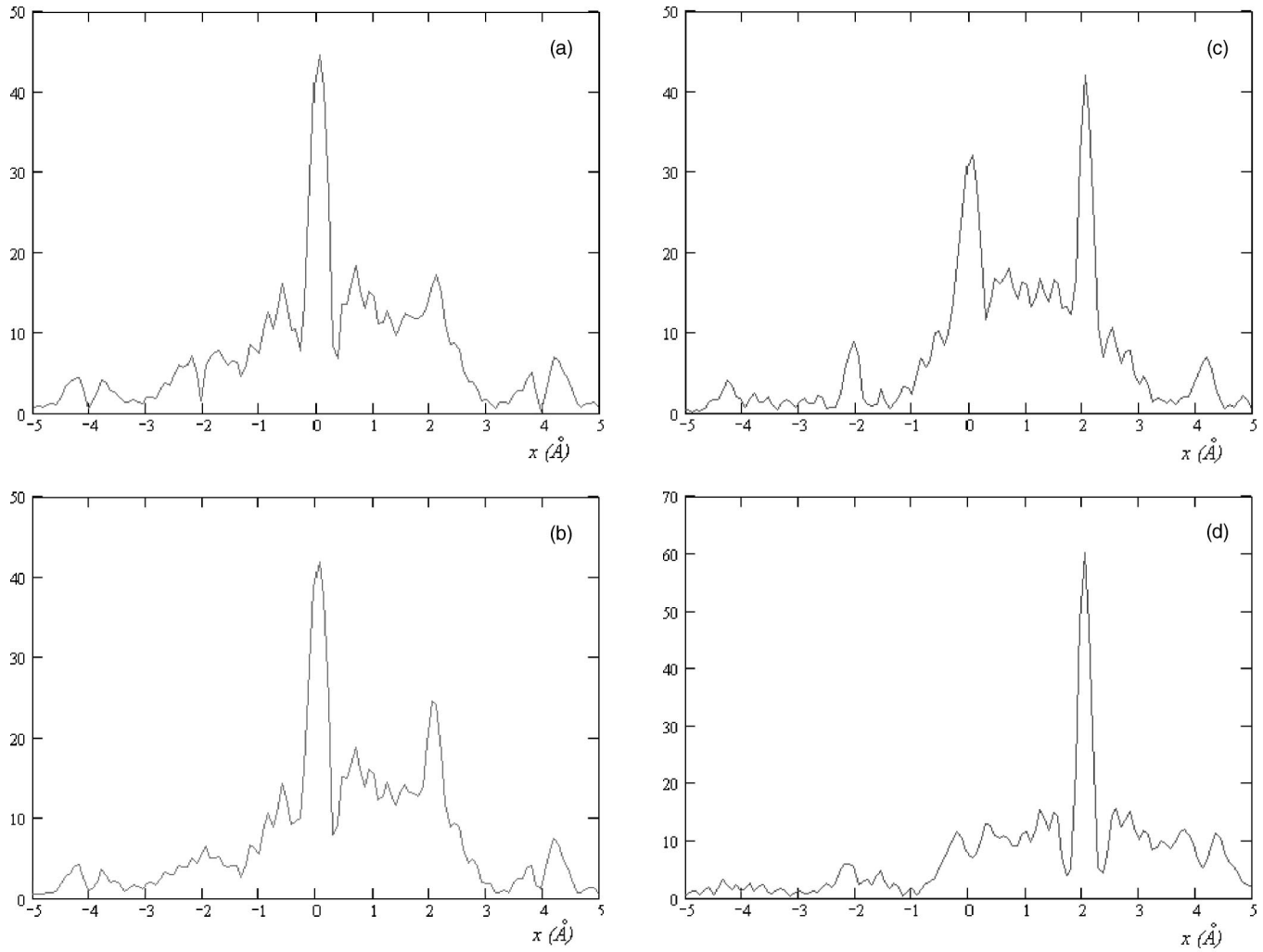

FIG. 8. (a)–(d) Atomic-focuser source produced by an incident beam with displacements 0.025, 0.05, 0.10, and 0.20 nm along the [001] crystal direction. 1D scans.

distance R between the source and the specimen. If this distance is not determined by the experimental arrangement, its value may be determined roughly from the magnification of the hologram image and refined by reconstructing with a range of values using the image sharpness as a criterion.

If the movement of the incident STEM beam exceeds half the separation of the atomic rows in the focuser crystal, the reconstructed image is repeated with the periodicity of the crystal projection, as in Figs. 9 and 10. If the displacement is not too great, the reconstruction can be considered as given by convoluting the true image with a function consisting of a central sharp peak and subsidiary, weaker peaks separated by the lattice vectors. If the subsidiary peaks are sufficiently small, the Fourier transform of this function does not approach zero at any point. It is then possible to remove the effects of the beam motion by deconvoluting, to retrieve the image function without ambiguity.

The minimum diameter of the region to be imaged is determined by the parameter R, since the attainment of ultrahigh resolution depends on the interference of scattered beams with a certain minimum angular spread. Thus for a resolution of 0.05 nm for 100 keV electrons, an angular range of about 10^{-1} rad is necessary, suggesting an image diameter of greater than 10 nm for a distance $R=100$ nm. The maximum diameter of the imaged region is limited only by the capability of the recording system and the computer used for the reconstruction to handle the number of pixels in the recorded hologram. It may be noted, however, that the value of the distance R that may be used may be limited in practice by the limitations of the available electron current. Since the energy incident on each element of the specimen (0.05 nm in diameter) decreases as $1/R^2$, the signal-to-noise ratio may become too small for large R values.

As with all in-line holography schemes, the reconstructed image is accompanied by the defocused conjugate image, the third term of Eq. (2.3), and the background from the first and fourth terms of Fig. 6. The contributions of these terms can be recognized in the reconstructions of Figs. 5 and 7. We suggest that these unwanted contributions may be removed by application of the well-known principles of off-axis holography, as commonly applied to TEM imaging.[8] If an electrostatic beam splitter in inserted in the illuminating system of the STEM instrument of Fig. 1, the atomic-focuser crystal

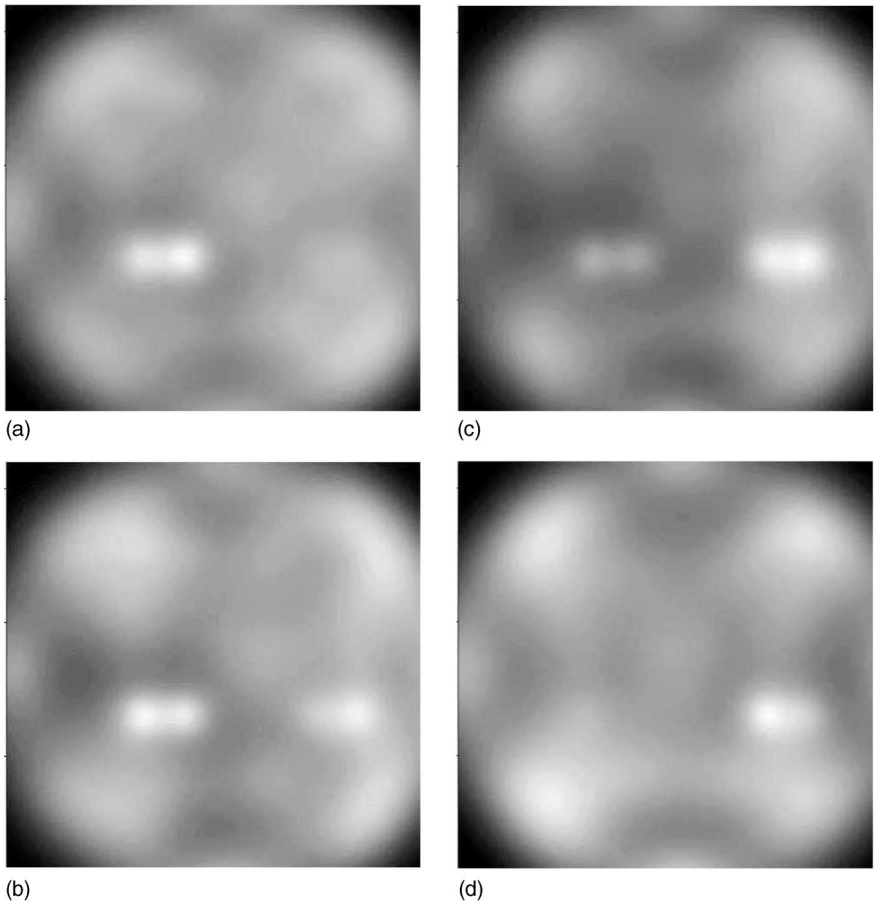

FIG. 9. (a)–(d) Images corresponding to a separation between specimen centers 0.05 nm for the cases of illumination by the atomic-focuser sources shown on Fig. 8.

is illuminated by two mutually coherent probes which have a variable separation A.[9] If both probes are channeled along lines of atoms in the crystal, the single source for the holography, $t(x)$, is replaced by $t(x)+t_0(x-A)$, where $t_0(x)$ has approximately the same dimensions and is similar to, but not necessarily identical with, $t(x)$. If the radiation from $t_0(x-A)$ does not pass through the specimen, it may serve as a reference beam and the intensity distribution of the hologram:

$$I_1(X)=|T_0(X/R\lambda)\exp(2\pi iAX/R\lambda)+q(X)\otimes t(X)\otimes g(X)|^2. \tag{7.1}$$

Thus the hologram is crossed by sinusoidal fringes with periodicity $X=R\lambda/A$. As in the usual off-axis TEM holography scheme,[8] the intensity distribution, Eq. (7.1), may be subjected to an imaging process consisting of the Fourier transform to give the diffraction pattern which is then modified and backtransformed. The diffraction pattern consists of a central region and two sidebands which arise from the cross-product terms of the square in Eq. (7.1). One of the sidebands is selected by use of an aperture and backtransformed to give the distribution.

$$T_0(X/R\lambda)[q(X)\otimes t(X)\otimes g(X)]. \tag{7.2}$$

If the specimen is small, only a few nm in diameter, $T_0(X/R\lambda)$ may be assumed to be unity for the region of interest, so that the reconstruction process can be carried out as for the pure in-line holography, as described above, to give the reconstructed image as

$$q(X)\otimes t(X).$$

Hence the constant background, the conjugate image, and the term of second order in $q(X)$ are removed. The object transmission function is imaged with a resolution given by the width of $t(X)$. The only limitation on the specimen is that

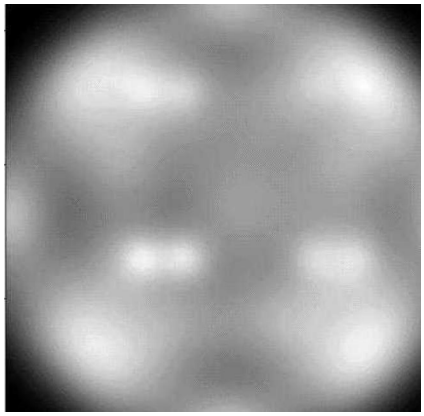

FIG. 10. Image corresponding to a separation of 0.05 nm between specimen centers, 0.05 nm for the case of illumination by an atomic focuser source produced with an incident beam oscillating with an amplitude of 0.05 nm. The image is repeated weakly with a periodicity of about 0.2 nm because the incident beam overlaps slightly the neighboring atomic columns of the crystal.

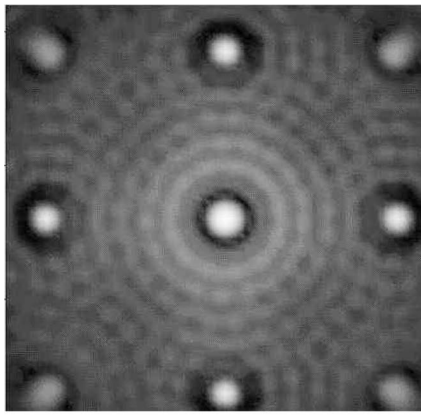

(a)

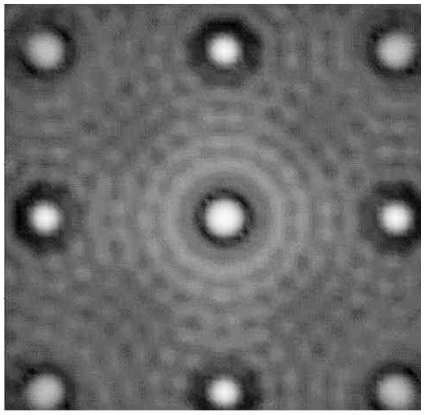

(b)

FIG. 11. Atomic-focuser sources produced by an incident beam with convergence angles 5 mrad (a), 4 mrad (b).

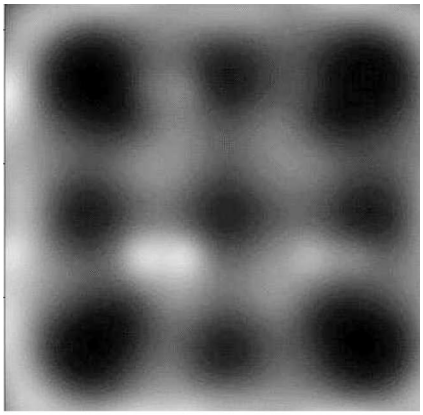

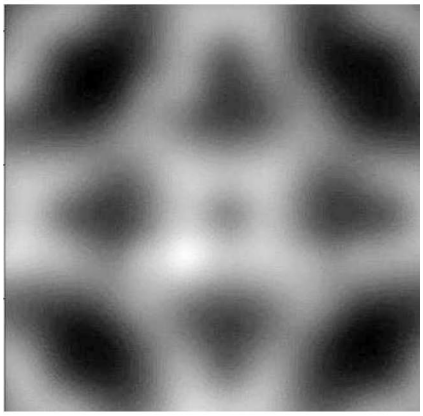

FIG. 12. Images corresponding to a separation between specimen centers of 0.05 nm for the illumination sources shown in Fig. 11.

it should be thin enough to allow its effect on the incident beam to be represented by a two-dimensional transmission function.

In the case that the object represented by $q(X)$ has dimensions less than $(R\lambda)^{1/2}$, it may be shown that the reconstruction from Eq. (7.2) can be reduced to

$$t_0^*(X) \otimes t(X) \otimes q(X), \tag{7.3}$$

so that, if $t_0(X)$ is identical to $t(X)$ and the corresponding transfer functions represent phase changes only (i.e., there is negligible absorption in the crystal), the first convolution of Eq. (7.3) gives a δ function and $q(X)$ is imaged with no resolution limitation.

The remaining difficulty for the practical application of the methods we have described is the experimental one of setting up a suitable thin crystal in an axial orientation and placing the specimen at an appropriate distance from the crystal. There is no requirement that the separation between the specimen and the crystal should have a particular value.[10] The only restriction is that it should lie within an appropriate range (e.g., between 10 and 100 nm for 100 keV electrons). The intensity in the hologram is almost equal to that in a normal shadow image obtained with a STEM beam of diameter about 0.2 nm and experience shows that such an image, with low noise, can be recorded within 1 sec or less.

In principle, the reconstruction from the in-line hologram could involve the correction for the aberrations of the atomic-focuser lens which could presumably be determined from the known potential distribution of the atoms concerned. However, there seems to be little incentive for the additional work involved in making such corrections since the improved resolution figures would be less than the diameters of the projected potential peaks for most atoms.

ACKNOWLEDGMENTS

We are grateful for the use of the facilities of the Center for High Resolution Electron Microscopy at Arizona State University, the assistance of Christoph Koch in computer programming, and the support of an Expert Visit Grant from the NATO Science Program.

*Electronic address: smir@paloma.spbu.ru

[1] D. Gabor, Nature (London) **161**, 777 (1948).
[2] D. Gabor, Proc. R. Soc. London, Ser. A **197**, 454 (1949).
[3] J.M. Cowley and D.J. Walker, Ultramicroscopy **6**, 71 (1981).
[4] J.A. Lin and J.M. Cowley, Ultramicroscopy **19**, 179 (1986).
[5] V.V. Smirnov, J. Phys. D **31**, 1548 (1998).

[6] J.M. Cowley, J.C.H. Spence, and V.V. Smirnov, Ultramicroscopy **68**, 135 (1997).
[7] M. Sanchez and J.M. Cowley, Ultramicroscopy **72**, 213 (1998).
[8] *Introduction to Electron Holography*, edited by E. Volkl, L. F. Allard, and D. C. Joy (Kluwer Academic, New York, 1998).
[9] J.M. Cowley, Ultramicroscopy **41**, 335 (1992).
[10] J.M. Cowley, Ultramicroscopy **81**, 47 (2000).